DYNAMICAL MONTHLY FORECASTING FOR AUSTRALIA: BRIDGING THE GAP BETWEEN WEATHER AND SEASONAL FORECASTING

Debbie Hudson* and Oscar Alves
Centre for Australian Weather and Climate Research (CAWCR), Bureau of Meteorology, Melbourne

1. INTRODUCTION

There is a growing trend towards seamless prediction: incorporating weather, medium-range, seasonal and ultimately climate change prediction in the same ensemble forecasting system (Dole, 2006; Palmer et al. 2008; Vitart et al. 2008). This is indeed the goal of the Bureau of Meteorology (BoM) with the development of the new Australian Community and Earth System Simulator (ACCESS, Puri, 2006).

Currently at the BoM, dynamical seasonal and interannual prediction is based on the Predictive Ocean Atmosphere Model for Australia (POAMA) (http://poama.bom.gov.au). Until recently it has not been possible to use POAMA for intra-seasonal or monthly forecasting. This is because for the retrospective forecasts (or hindcasts), the atmosphere and land components of the dynamical model were initialized from an AMIP-style atmosphere-only simulation. Thus, the initial conditions contained observed atmospheric and land information which is related to sea-surface temperature, but they did not capture the true intra-seasonal state. However, the Centre for Australian Weather and Climate Research (CAWCR) has recently introduced a new version of POAMA (Wang et al., 2008) which incorporates a new Atmosphere and Land Initialisation (ALI) scheme, developed as part of the ACCESS project (Hudson and Alves, 2007). This new system has the potential to bridge the gap between weather and seasonal forecasting, since forecasts in the 10-60 day range are influenced by initial conditions of the atmosphere and land, as well as the ocean. The subseasonal scale, particularly from the second week to the first month of the forecast, is, however, notoriously difficult to predict.

In this paper, we examine the intra-seasonal forecast skill of our hindcast dataset, focusing on minimum and maximum temperatures and precipitation over Australia.

---

* *Corresponding author address*: Debbie Hudson, CAWCR, Bureau of Meteorology, GPO Box 1289, Melbourne, 3001, Australia; email: D.Hudson@bom.gov.au

2. POAMA MODEL & HINDCAST DATASET

The atmospheric model component of POAMA is the BoM's atmospheric model (BAM version 3.0; Colman et al. 2005; Wang et al. 2005; Zhong et al. 2006) which has a T47 horizontal resolution and 17 levels in the vertical. The land surface component is a simple bucket model for soil moisture (Manabe and Holloway 1975) and has three soil levels for temperature. The ocean model is the Australian Community Ocean Model version 2 (ACOM2; Schiller et al. 2002), and is based on the Geophysical Fluid Dynamics Laboratory Modular Ocean Model (MOM version 2). The ocean grid resolution is 2º in the zonal direction and in the meridional direction it is 0.5º at the equator and gradually increases to 1.5º near the poles. The atmosphere and ocean models are coupled using the Ocean Atmosphere Sea Ice Soil (OASIS) coupling software (Valcke et al. 2000). The ocean data assimilation scheme is based on the optimum interpolation technique of Smith et al (1991).

This study uses version 1.5 of POAMA (operational at BoM since January 2008) which obtains atmospheric initial conditions from the previously mentioned ALI scheme (Hudson and Alves, 2007). ALI involves the creation a new reanalysis dataset using the atmospheric model of POAMA. The scheme generates realistic atmospheric initial conditions, as well as land surface initial conditions that are in balance with this atmospheric forcing.

The hindcast dataset used is a 10-member ensemble, with forecasts of 9 months duration, starting on the first day of every month for 1980 to 2005. For any given start month for each of these years, a lead-time dependent ensemble mean and model climatology is created. The ensemble mean forecast (or individual ensemble member) is compared against this climatology to create anomalies, and in so doing a first-order linear correction for model bias or drift is made

3. INTRASEASONAL SKILL

Here we assess the skill of POAMA in predicting the first and second fortnight of the forecast (average of days 1-14 and 15-28). Since POAMA uses realistic atmospheric (although degraded compared to that used in NWP) and ocean initial conditions the skill of forecasts for the first week is high. However, after the first week the spread of the ensemble is large and the forecasts are inherently probabilistic. We thus focus on probabilistic forecasts of exceeding tercile thresholds and use the relative operating characteristic (ROC) area and ROC curve for verification (e.g. Mason and Graham, 1999; Joliffe and Stephenson, 2003). For calculation of the tercile thresholds we use data for all years except the one under consideration (leave-one-out cross validation). ROC curves provide information on forecast resolution by measuring the ability of a forecast to discriminate between the occurrence and non-occurrence of an event. We also show some deterministic verification in the form of anomaly correlation. The BoM high quality gridded data were used for the observed data.

3.1 Precipitation

Figure 1 shows the anomaly correlation skill for precipitation for the first and second fortnights for all forecast start months. The degradation in skill in the second half of the month is very clear, and most of the skill in the first fortnight comes from the first week of the forecast. Skill in the second fortnight varies a great deal as a function of region and forecast start month. It is highest over south-eastern Australia and in the months from July to October (JASO) (Figure 2).

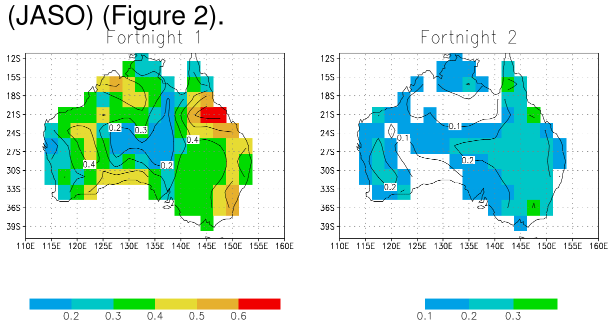

Fig. 1: Precipitation anomaly correlation for all forecast start months for the first and second fortnights of the forecast. Significant correlations are shaded (t-test, n=312, r>0.1 is significant at p=0.05).

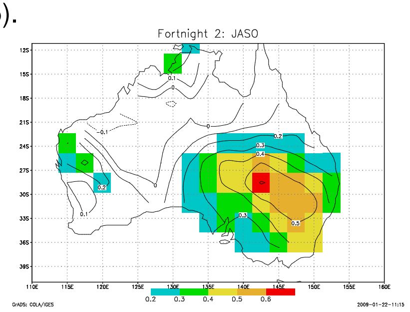

Fig. 2: Precipitation anomaly correlation for July, August, September and October forecast start months for the second fortnight of the forecast. Significant correlations are shaded (t-test, n=104, r>0.19 is significant at p=0.05).

Figure 3 shows the ROC score (normalised area under the ROC curve) of the probability that precipitation averaged over the second fortnight is in the lower or upper tercile for the same forecast start months (JASO). Again the skill over the south-east is apparent. The model appears to be slightly better at forecasting events falling in the upper tercile than in the lower tercile. For both categories, much of the south-east has skill greater than the climatological value of 0.5. In addition, the model performs significantly better in the second fortnight compared to persisting forecast probabilities of the first fortnight.

ROC curves for the south-east are displayed in Figure 4. For skilful forecasts the ROC curve bends towards the top left corner of the plot, where hit rates exceed false alarm rates. A curve lying close to the diagonal (i.e. ROC area≈0.5) has little skill and one lying below the diagonal has negative skill (i.e. ROC area<0.5). The curves in Figure 4 show the decline in skill from the first to the second fortnight, with useful skill still prevailing in the latter. As shown in Figure 3, the model provides more skill in the second fortnight than simply persisting the forecast from the first fortnight (Figure 4).

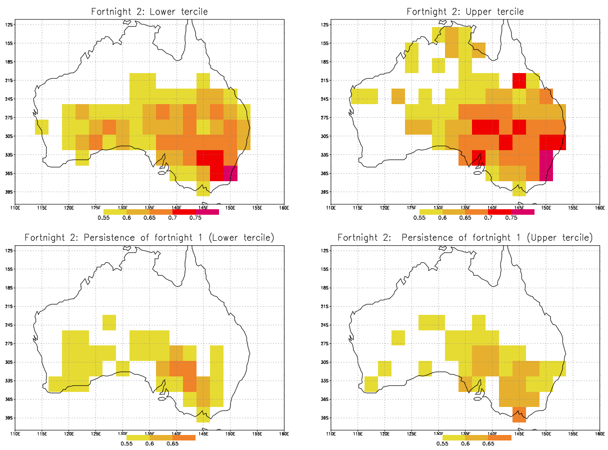

Fig. 3: ROC area (score) of the probability that precipitation averaged over the second fortnight is in the lower (left) or upper (right) tercile for July, August, September and October forecast start months. ROC scores above 0.55 are shown. The lower panel shows the ROC areas obtained by persisting the probabilities from the first fortnight.

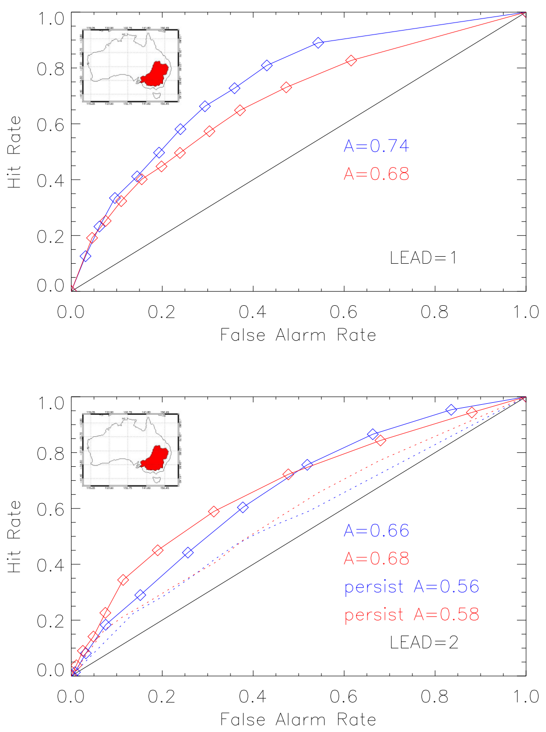

Fig. 4: ROC curves of the probability that precipitation averaged over the first (top) and second fortnights (bottom) is in the upper (red) or lower (blue) tercile. The dotted lines in the second fortnight plot are the ROC curves obtained by persisting the probabilities from the first fortnight. The ROC score, or area under each ROC curve (A) is also shown. ROC curves are obtained from July, August, September and October forecast start months for the south-east of Australia (map inset).

3.2 Maximum Temperature

Anomaly correlation skill for maximum temperature is generally higher than that for precipitation, particularly for the first fortnight (Figure 5). For the second fortnight, skill is greatest in the latter half of the year and is focussed on the south-east, e.g. see Figure 6 for forecast start months August, September, October and November (ASON).

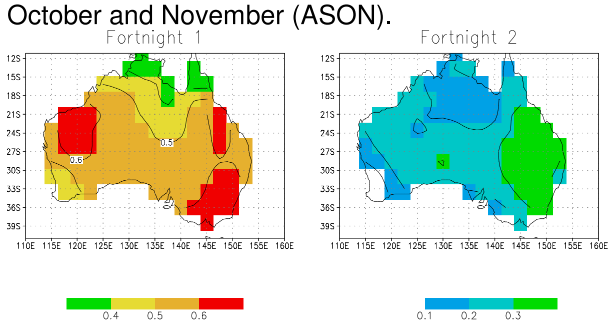

Fig. 5: Maximum temperature anomaly correlation for all forecast start months for the first and second fortnights of the forecast. Significant correlations are shaded (t-test, n=312, r>0.1 is significant at p=0.05).

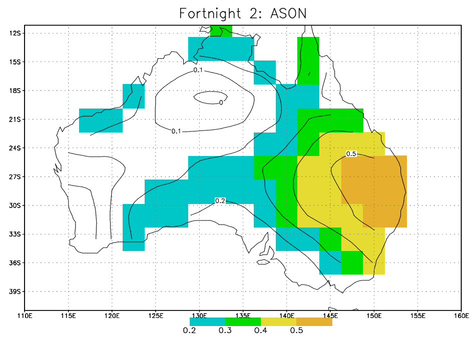

Fig. 6: Maximum temperature anomaly correlation for August, September, October and November forecast start months for the second fortnight of the forecast. Significant correlations are shaded (t-test, n=104, r>0.19 is significant at p=0.05).

The ROC scores for maximum temperature falling in the upper tercile shows some useful skill for forecast start months ASON (Figures 7 and 8). Over the eastern part of Australia the ROC score exceeds 0.5, suggesting that the model performs better than climatology. In addition, for the second fortnight, the model provides more skill than just persisting the forecast probabilities from the first fortnight (Figures 7 and 8).

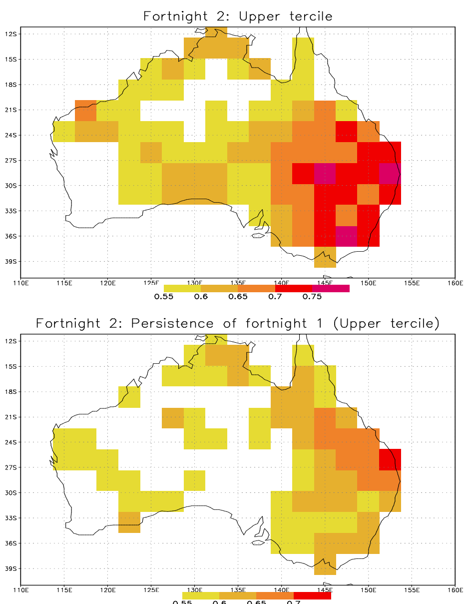

Fig. 7: ROC area (score) of the probability that maximum temperature averaged over the second fortnight is in the upper tercile for August, September, October and November forecast start months. ROC scores above 0.55 are shown. The lower panel shows the ROC areas obtained by persisting the probabilities from the first fortnight.

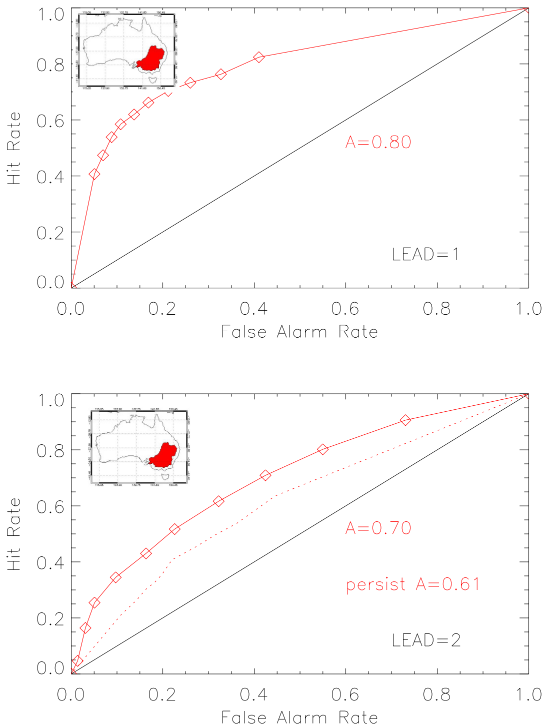

Fig. 8: ROC curves of the probability that maximum temperature averaged over the first (top) and second fortnights (bottom) is in the upper tercile. The dotted line in the second fortnight plot is the ROC curve obtained by persisting the probabilities from the first fortnight. The ROC score, or area under each ROC curve (A) is also shown. ROC curves are obtained from August, September, October and November forecast start months for the south-east of Australia (map inset).

3.3 Minimum Temperature

Of the three variables analysed, minimum temperature is the least skilful, particularly for the second fortnight (Figure 9). This is also true for the probabilistic forecasts (not shown).

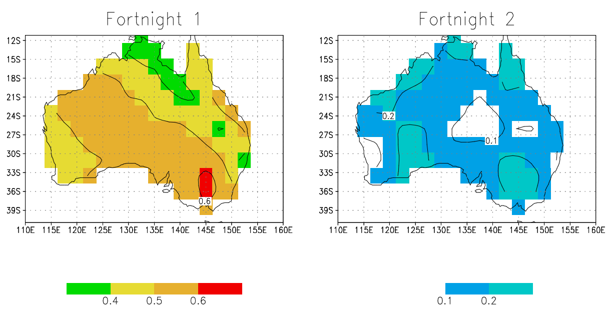

Fig. 9: Minimum temperature anomaly correlation for all forecast start months for the first and second fortnights of the forecast. Significant correlations are shaded (t-test, n=312, r>0.1 is significant at p=0.05).

4. CASE STUDIES

We have shown that the model has some skill in predicting the second fortnight of the forecast. The question is, when the model gets it correct, is it getting it right for the correct synoptic reasons? Under what circumstances does the model produce a good forecast? In the presentation we analyse some case studies in an attempt to answer some of these questions.

5. CONCLUSIONS

This initial examination of intra-seasonal skill of POAMA is promising. There are definite indications of useful skill for certain regions at certain times of the year. Over south-eastern Australia, for the forecast of the second fortnight (average days 15-28) the model performs generally better than the persistence of probabilities from the first fortnight (average days 1-14) and better than climatology. The model seems less skilful for minimum temperature compared to either maximum temperature or precipitation.

The next version of POAMA may provide some improvements in skill, since it has a higher atmospheric model resolution (T63). Perhaps more importantly, the new hindcast dataset planned for the next version will be designed to incorporate intra-seasonal prediction (one forecast start date per month, as in the current hindcast set, is not sufficient).

A significant limitation of the current version of POAMA is its simple land surface model. There may be benefits for intra-seasonal forecasting from improving the initialisation and simulation of the land surface, primarily due to soil moisture memory in the earth-atmosphere system. Here we are hoping that the future transition to the ACCESS model, which has the more complex and flexible CABLE land surface model, will be advantageous for intra-seasonal and seasonal prediction.

6. REFERENCES

Colman, R., Deschamps, L., Naughton, M., Rikus, L., Sulaiman, A., Puri, K., Roff, G., Sun, Z., and Embery, G., 2005: BMRC Atmospheric Model (BAM) version3.0: comparison with mean climatology. BMRC Research Report No. 108. Bureau of Meteorology.

Dole, R.M., 2006: Linking Weather and Climate. *Science and Technology Infusion Climate Bulletin (NOAA)*. July 2006.

Hudson, D. and Alves, O. 2007: The impact of land-atmosphere initialisation on dynamical seasonal prediction. BMRC Research Report No. 133, Bureau of Meteorology, p19-22

Manabe, S. and Holloway, J., 1975: The seasonal variation of the hydrological cycle as simulated by a global model of the atmosphere. *Journal of Geophysical Research*, 80, 1617-1649.

Mason, S.J. and Graham, N.E. 1999: Conditional Probabilities, Relative Operating Characteristics, and Relative Operating Levels. *Weather and Forecasting*, 14, 713-725.

Joliffe, I.T. and Stephenson, D.B., 2003: *Forecast Verification: A Practitioner's Guide in Atmospheric Science.* Wiley, New York.

Palmer, T.N., Doblas-Reyes, F.J., Weisheimer, A. and Rodwell, M.J., 2008: Toward Seamless Prediction: Calibration of Climate Change Projections using Seasonal Forecasts. *Bull. Am. Met. Soc.*, 89, 459-470.

Puri 2006: Overview of ACCESS. BMRC Research Report No. 123, Bureau of Meteorology Research Centre, p1-4

Schiller, A., Godfrey, J.S., McIntosh, P.C., Meyers, G., Smith, N.R., Alves, O., Wang, G. and R. Fiedler, 2002: A New Version of the Australian Community Ocean Model for Seasonal Climate Prediction. CSIRO Marine Research Report No. 240, 82 pp.

Smith, N.R., Blomley, J.E. & Meyers, G., 1991: A univariate statistical interpolation scheme for subsurface thermal analyses in the tropical oceans. *Progress In Oceanography*, 28(3), p.219-256.

Valcke, S., Terray, L. and Piacentini, A., 2000: Oasis 2.4, Ocean atmosphere sea ice soil: user's guide. TR/CMGC/00/10, CERFACS, Toulouse, France.

Vitart, F., Buizza, R., Balmaseda, M.A., Balsamo, G., Bidlot, J-R., Bonet, A., Fuentes, M., Hofstadler, A., Molteni, F. and Palmer, T.N. 2008: The new VarEPS-monthly forecasting system: A first step towards seamless prediction. *Q. J. Royal Met. Soc.*, 134, 1789-1799.

Wang, G., Alves, O. and Smith, N., 2005: BAM3.0 tropical surface flux simulation and its impact on SST drift in a coupled model. BMRC Research Report No. 107, Bureau of Meteorology.

Wang, G., Alves,O., Hudson, D., Hendon, H.,Liu, G. and Tseitkin, F., 2008: SST Skill Assessment from the new POAMA-1.5 system. *BMRC Research Letter*, 8, 1–6.

Zhong, A., Alves, O., Hendon, H. and Rikus, L., 2006: On aspects of the mean climatology and tropical interannual variability in the BMRC Atmospheric Model (BAM 3.0). BMRC Research Report No. 121, Bureau of Meteorology.